Discovery of Novel Bromate−Sulfite pH Oscillators with Mn^{2+} or MnO_4^- as a Negative-Feedback Species

Noriaki Okazaki, Gyula Rábai,† and Ichiro Hanazaki*

Department of Chemistry, Faculty of Science, Hiroshima University, 1-3-1 Kagamiyama, Higashi-Hiroshima 739-8526, Japan

Received: July 27, 1999; In Final Form: October 5, 1999

A novel pH oscillator has been constructed by combining the pH clock reaction system BrO_3^-−SO_3^{2-}−H^+ with Mn^{2+} as a proton-consuming species. The system exhibits large-amplitude pH oscillations typically between pH = 2.8 and pH = 7.3 at 45 °C in a continuous-flow stirred tank reactor. The oscillatory waveform is similar to that of a pulse wave, and the duration of both high-pH and low-pH stages can be changed in a wide range by controlling the input concentrations of BrO_3^- and Mn^{2+}. The state diagram spanned by the input concentrations of BrO_3^- and Mn^{2+} takes the form of a cross-shaped diagram. It has been found that MnO_4^-, in place of Mn^{2+}, is also effective in consuming H^+ to give large-amplitude pH oscillations. A possible reaction mechanism for the removal of H^+ has been discussed in which $MnO(OH)^+$ is reduced by HSO_3^- to give $HS_2O_6^-$. This properly accounts for the stoichiometry for both the Mn^{2+} and MnO_4^- systems. The proposed reaction scheme is unique among pH oscillators reported so far in that the sulfite ion plays a key role in both the nonlinear production and consumption of protons.

Introduction

Since the first discovery of large-amplitude pH oscillations in the reaction of hydrogen peroxide with sulfide ion,[1] a number of pH oscillators have been discovered, which now constitute a large family of pH-regulated chemical oscillators.[2] The common feature shared among the pH oscillators is that they involve an autocatalytic production of H^+ (positive feedback) and a H^+-consuming pathway (negative feedback) in their reaction networks. The scheme was summarized in an abstract model and was successfully utilized as a guiding principle for the systematic design of novel pH oscillators.[2,3] Spatial pattern formation[4−7] and photoresponse[8−13] were studied for a number of pH oscillators. Recently, the idea of simultaneous employment of two negative-feedback species led to the discovery of chaotic pH oscillations,[14−16] for which photoinduced bifurcation to chaos was demonstrated for the first time.[17] Although most of the studies of the pH oscillators reported so far have been more or less kinetics-oriented, practical applications of the pH oscillators to the temporally controlled drug delivery system[18−20] and to the control medium for the rhythmically pulsatile mechanical motion of a polymer hydrogel system emulating muscular tissue[21] have also been suggested.

The BrO_3^-−SO_3^{2-}−H^+ (BSH) system is known to exhibit clock-reaction behavior in a batch reactor and bistability in a continuous-flow stirred tank reactor (CSTR) because of the autocatalytic multiplication of H^+ involved in the reaction. The system shows large-amplitude pH oscillations when combined with a negative-feedback species such as $Fe(CN)_6^{4-}$.[22] The reaction mechanism for this system originally postulated by Edblom et al.[22] was recently reexamined by Rábai et al.[23] (RKH). They proposed an alternative model[23,24] featuring the old work of Williamson and King[25] which was shown to better describe many aspects of the observed behavior.[26] Hanazaki and Rábai[24] further simplified the RKH mechanism to give a three-variable model, for which the origin of chemical instability was mathematically analyzed.

In the following, a brief description of the reaction in the BSH system will be given based on the RKH mechanism.[23,24] The whole reaction is composed of two sets of reaction channels. The first set consists of the reactions of HSO_3^- (the S channel),

$$H^+ + SO_3^{2-} \leftrightarrow HSO_3^- \qquad \text{(SE)}$$

$$HSO_3^- + BrO_3^- \rightarrow SO_4^{2-} + HBrO_2 \qquad \text{(S1)}$$

$$HSO_3^- + HBrO_2 \rightarrow SO_4^{2-} + HOBr + H^+ \qquad \text{(S2)}$$

$$HSO_3^- + HOBr \rightarrow SO_4^{2-} + Br^- + 2H^+ \qquad \text{(S3)}$$

and the second set consists of the reaction of H_2SO_3 (the D channel),

$$H^+ + HSO_3^- \leftrightarrow H_2SO_3 \qquad \text{(DE)}$$

$$H_2SO_3 + BrO_3^- \rightarrow SO_4^{2-} + HBrO_2 + H^+ \qquad \text{(D1)}$$

$$H_2SO_3 + HBrO_2 \rightarrow SO_4^{2-} + HOBr + 2H^+ \qquad \text{(D2)}$$

$$H_2SO_3 + HOBr \rightarrow SO_4^{2-} + Br^- + 3H^+ \qquad \text{(D3)}$$

The clock-reaction behavior in a batch reactor can be explained as follows. Reactions SE and DE are rapid equilibria. The equilibrium constant for reaction SE is extremely large so that in excess of SO_3^{2-} practically no H^+ is existent in the system. Reactions S1−S3 produce H^+, which is, however, consumed instantaneously by SO_3^{2-} through reaction SE. The net result

* To whom correspondence should be addressed. E-mail: hanazaki@sci.hiroshima-u.ac.jp.

† On leave from Institute of Physical Chemistry, Kossuth Lajos University, H-4010 Debrecen, Hungary.

10.1021/jp992626l CCC: $18.00
Published on Web 11/19/1999

is that $[H^+] \approx 0$ throughout and $[SO_3^{2-}]$ decreases gradually. This continues up to the complete consumption of SO_3^{2-}, giving rise to the induction period. The sum (reaction SE) + (reaction S1) + (reaction S2) + (reaction S3) gives the overall reaction

$$3H^+ + 3SO_3^{2-} + BrO_3^- \rightarrow 3SO_4^{2-} + Br^- + 3H^+ \quad (S)$$

which is catalytic but not autocatalytic with respect to H^+. The rate-determining step of the S channel is considered to be step S1. During the induction period, $[H_2SO_3] \approx 0$ by reaction DE, since $[H^+] \approx 0$, and the D channel reaction never takes place. When SO_3^{2-} is consumed completely, H^+ starts to be liberated to give a nonzero value of $[H_2SO_3]$ according to reaction DE. Then the D channel reaction sets in, where the total stoichiometry is (DE) + (D1) + (D2) + (D3):

$$3H^+ + 3HSO_3^- + BrO_3^- \rightarrow 3SO_4^{2-} + Br^- + 6H^+ \quad (D)$$

This process is autocatalytic with respect to H^+, giving rise to a sharp increase of $[H^+]$ and therefore a sharp decrease of pH.

Hanazaki and Rábai[24] have further shown theoretically that the BSH system should exhibit large-amplitude pH oscillations when combined with an appropriate first-order H^+-consuming process. On the basis of this prediction, it has experimentally been shown that $CaCO_3$ contained in marble removes H^+ selectively.[27] However, the species known so far to be effective in the negative-feedback process is limited; only $Fe(CN)_6^{4-}$ and $CaCO_3$ in marble are known, which is much restricted compared with the case of the analogous system, $IO_3^- - SO_3^{2-} - H^+$.[2] This is an unfortunate situation for the realistic application of the BSH system, particularly if one considers the harmfulness of $Fe(CN)_6^{4-}$ and an additional difficulty brought about by the solid−liquid interface in the case of marble. In this context, it is highly desirable to find new negative-feedback species for the BSH system that can feasibly be handled.

In this study, we report on the large-amplitude pH oscillations discovered in the BSH system combined with a novel negative-feedback species Mn^{2+}. The system behavior has been thoroughly examined on the control-parameter plane spanned by the input concentrations of BrO_3^- and Mn^{2+}, based on which a possible mechanism relevant for the H^+ consumption is discussed. In addition, we have found that the permanganate ion, MnO_4^-, is also effective as a negative-feedback source in place of Mn^{2+}. In this paper, we try to establish a universal reaction scheme for these two pH oscillator systems.

Experimental Section

Reagent-grade chemicals Na_2SO_3, $HClO_4$, $MnSO_4 \cdot 5H_2O$ (Kanto Chemical), $KMnO_4$ (Katayama Chemical), and $NaBrO_3$ (Kishida Chemical) were used without further purification. The purity of Na_2SO_3 and the molarity of $HClO_4$ were analyzed by iodine titration. The $MnSO_4$ content was determined by EDTA titration. Throughout the experiment, ultrapure water supplied by a water purification system (Millipore, Milli-Q Jr.) was used as solvent. The stock solutions of Na_2SO_3 and $MnSO_4$ were prepared daily and were continuously bubbled with N_2 in order to avoid possible air oxidation.

The experiment was carried out in a CSTR configuration as described elsewhere.[28] A water-jacketed quartz-glass beaker was used as a reactor. Four stock solutions, each containing SO_3^{2-}, H^+, Mn^{2+}, and BrO_3^-, respectively, were separately introduced into the reactor by a peristaltic pump (EYELA, MP-3S) through glass capillary tubes. The reaction mixture was vigorously stirred by a Teflon coated magnetic stirrer bar. The volume of the mixture in the reactor was kept at 9.0 mL by continuous aspiration of solution from the top of the reactor. The reaction temperature was maintained at 45.00 ± 0.05 °C by circulating water between the water jacket and a thermostated water bath (EYELA, NTT-1200). The system pH was monitored by a calibrated glass electrode (Horiba, 6861-10C) vertically inserted in the reactor and was recorded by a personal computer through a pH meter (Horiba, D-10) and a 12-bit A/D converter (CONTEC, AD12-16LG(PC)) with a sampling rate of 2 Hz.

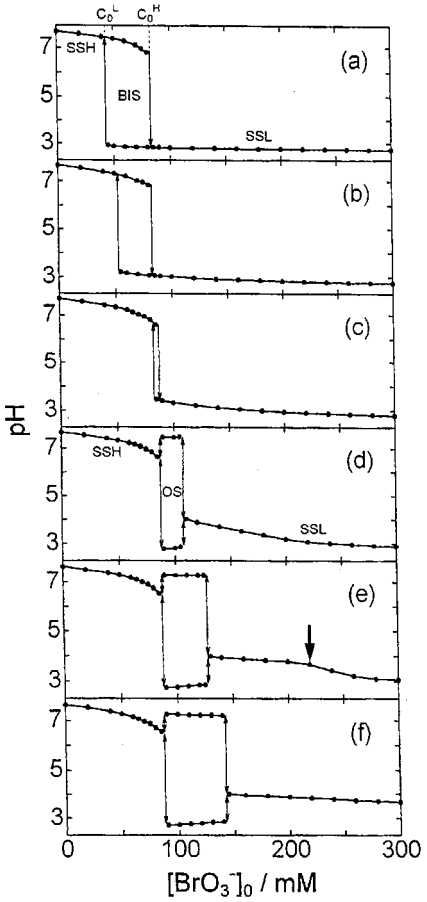

Figure 1. Bifurcation diagrams in the $Mn^{2+} - BrO_3^- - SO_3^{2-} - H^+$ system obtained for the following various $[Mn^{2+}]_0$: (a) 0.0, (b) 1.8, (c) 3.6, (d) 5.4, (e) 7.2, and (f) 9.0 mM. The constraint parameter is $[BrO_3^-]_0$, and the response variable is pH. The labels SSH, SSL, BIS, and OS stand for the high-pH steady state, low-pH steady state, the bistability between SSH and SSL, and the oscillatory state, respectively. In OS, the peak and the valley of pH oscillations are plotted. The experimental conditions are $[H^+]_0 = 16.5$ mM, $[SO_3^{2-}]_0 = 118$ mM, temperature = 45.0 °C, and the residence time = 5.66 min.

Results and Discussion

For the $BrO_3^- - SO_3^{2-} - H^+ - Mn^{2+}$ system, the condition for stable pH oscillations was systematically searched for on the $[BrO_3^-]_0$-$[Mn^{2+}]_0$ control-parameter plane with other constraint parameters being fixed. Here, $[X]_0$ denotes the initial concentration of species X, which is defined as the concentration of X to be attained in the reactor if no reaction took place. In practice, the pH response due to the change of $[BrO_3^-]_0$ was examined for a given value of $[Mn^{2+}]_0$, and the measurement was repeated with varying $[Mn^{2+}]_0$ from 0 to 9 mM with a 1.8 mM step width. The results are summarized in a series of bifurcation diagrams as shown in Figure 1.

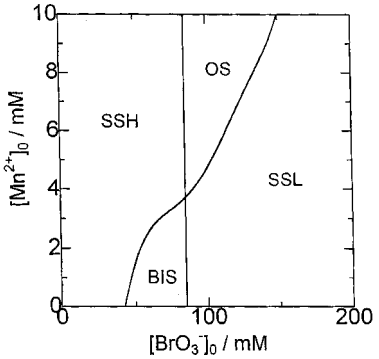

Figure 2. Cross-shaped phase diagram established on the control-parameter plane spanned by $[BrO_3^-]_0$ and $[Mn^{2+}]_0$. Labels SSH, SSL, BIS, and OS and the experimental conditions are the same as those given in Figure 1.

At $[Mn^{2+}]_0 = 0$ mM (Figure 1a), the system exhibits two stationary steady states, one with high pH (SSH) and the other with low pH (SSL). The SSH is stable at low $[BrO_3^-]_0$ and destabilizes above a critical concentration C_0^H. The SSL is stable for the high $[BrO_3^-]_0$ region and loses its stability below C_0^L. The solution is colorless for both steady states. The region of bistability between SSH and SSL is established in the range $C_0^L < [BrO_3^-]_0 < C_0^H$. In conventional terminology,[29] SSH is regarded as the "flow branch" in which autocatalysis of H^+ (D channel) is suppressed, since reaction S1 does not proceed quickly enough to consume SO_3^{2-} supplied by the inflow. On the other hand, SSL is the "thermodynamic branch" where the D channel is activated.

As can be seen in Figure 1, the addition of Mn^{2+} does not change the behavior of SSH and C_0^H remains almost constant irrespective of $[Mn^{2+}]_0$, indicating that Mn^{2+} is almost inert as to the reaction dynamics operating in SSH. On the other hand, the increase of $[Mn^{2+}]_0$ substantially increases pH in SSL especially when $[BrO_3^-]_0$ is lower. The slope $|\partial pH/\partial[BrO_3^-]_0|$ becomes steeper and the critical concentration C_0^L increases as $[Mn^{2+}]_0$ is increased. As a result, the bistable region shrinks with $[Mn^{2+}]_0$ and almost disappears around $[Mn^{2+}]_0 = 3.6$ mM. Further increase of $[Mn^{2+}]_0$ makes C_0^H surpass C_0^L.

In this higher $[Mn^{2+}]_0$ region (Figure 1d−f), the large-amplitude regular pH oscillations (OS) are observed in the range $C_0^H < [BrO_3^-]_0 < C_0^L$, where both SSH and SSL are unstable. The oscillatory amplitude exceeds 4 pH units and is almost independent of $[BrO_3^-]_0$. Within the present experimental resolution, no hysteresis has been detected for the transition between SSH and OS as well as for the transition between OS and SSL, although the transitions take place in a discontinuous manner. The oscillatory region broadens monotonically with $[Mn^{2+}]_0$ up to $[Mn^{2+}]_0 = 9$ mM. Thus, a typical "cross-shaped diagram"[30] is obtained on the control-parameter plane spanned by $[BrO_3^-]_0$ and $[Mn^{2+}]_0$ as shown in Figure 2.

In addition to the occurrence of pH oscillations, a notable feature appears in SSL at $[Mn^{2+}]_0 = 7.2$ mM; the pH response exhibits a kink at $[BrO_3^-]_0 \approx 220$ mM as marked by an arrow in Figure 1e. For $[BrO_3^-]_0 < 220$ mM, SSL shows little dependence on $[BrO_3^-]_0$ but is very sensitive to the external noise; the system is readily excited by a small perturbation such as a temporal stop of flow or stirring for few seconds. The excitability should be mainly due to the extinction of the D channel, but some additional nonlinearity other than the D channel may also operate. Note that an excitability has also been pointed out in the $Fe(CN)_6^{4-}-IO_3^--SO_3^{2-}-H^+$ system in the low-pH steady state close to the oscillatory state.[31] At $[Mn^{2+}]_0 = 9.0$ mM, SSL resides in the excitable state up to $[BrO_3^-]_0 = 300$ mM.

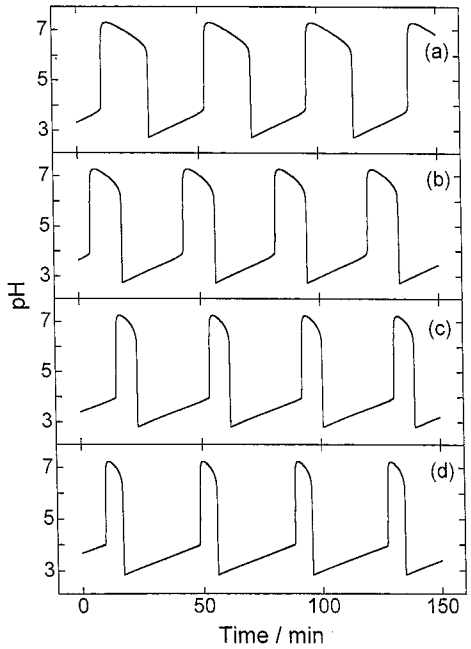

Figure 3. Measured pH oscillations for the following $[BrO_3^-]_0$: (a) 90, (b) 100, (c) 120, and (d) 130 mM. $[Mn^{2+}]_0$ is fixed at 9.0 mM. Other experimental conditions are the same as those given in Figure 1.

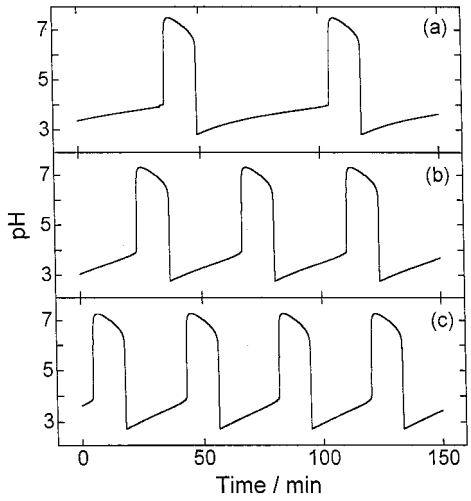

Figure 4. Measured pH oscillations for the following $[Mn^{2+}]_0$: (a) 5.4, (b) 7.2, and (c) 9.0 mM. $[BrO_3^-]_0$ is fixed at 100 mM. Other experimental conditions are the same as those given in Figure 1.

Figure 3 shows the waveform of pH oscillations and its variation with $[BrO_3^-]_0$ where $[Mn^{2+}]_0$ is fixed at 9.0 mM. The waveform exhibits typical relaxation oscillations characterized by the relatively slow pH change in both the low-pH and high-pH stages and rapid transitions between them. The solution is colorless, and no precipitate has been detected throughout the course of oscillations. The oscillation amplitude is as large as 4.5 pH units, one of the largest on record in the pH-oscillator family reported so far. The time duration of the high-pH stage decreases with $[BrO_3^-]_0$ steadily. On the other hand, the duration of the low-pH stage increases in proportion to $[BrO_3^-]_0$. The total oscillatory period is nearly independent of $[BrO_3^-]_0$. In Figure 4 the oscillatory waveforms are compared for various $[Mn^{2+}]_0$ with a fixed value of $[BrO_3^-]_0 = 100$ mM. Here, the duration of the low-pH stage decreases in proportion to

$1/[Mn^{2+}]_0$ while that of the high-pH stage is independent of $[Mn^{2+}]_0$. The total oscillatory period decreases with $[Mn^{2+}]_0$.

As shown in Introduction, the reaction kinetics of the $BrO_3^- - SO_3^{2-} - H^+$ subsystem is now well understood and we already have a reliable model that can quantitatively reproduce the clock-reaction behavior in a batch reactor as well as the bistability in a CSTR.[23−25,27] The experimental results presented here also support this model; the destabilization of SSH as well as the decrease in the high-pH duration of OS due to increasing $[BrO_3^-]_0$ can naturally be explained as a result of the enhanced rate of reaction S1, which is the rate-determining step in the S channel. The independence of the high-pH duration on $[Mn^{2+}]_0$ can also be understood if the system behavior here is solely determined by the S channel reactions, while manganese has nothing to do.

On the other hand, the reaction mechanism relevant to the removal of H^+ in the low-pH region of OS seems to require some discussion. One may naturally consider that Mn^{2+} is oxidized by BrO_3^- with a consumption of H^+ in the low-pH region. However, this scheme is unlikely to account for the observation, since the duration of the low-pH period increases with $[BrO_3^-]_0$. To account for this observation, we assume that the effective H^+ consumption takes place through the process in which an oxidized form of manganese species is reduced back to Mn^{2+} by HSO_3^-. The possible oxidation products of manganese that are stable at pH = 3−4 are $Mn(OH)^{2+}$, $Mn(OH)_2^{2+}$, and $MnO(OH)^+$.[32] Among them, we propose that $MnO(OH)^+$ should play the most important role, since it undergoes the reaction

$$MnO(OH)^+ + 2HSO_3^- + 2H^+ \rightarrow Mn^{2+} + HS_2O_6^- + 2H_2O \quad (1)$$

where $MnO(OH)^+$ may be produced from Mn^{2+} as follows:[32]

$$3Mn^{2+} + BrO_3^- + 3H_2O \rightarrow 3MnO(OH)^+ + Br^- + 3H^+ \quad (2)$$

In reaction 1, hexaoxodisulfate, $S_2O_6^{2-}$, has been assumed to play an important role. This is usually obtained by the oxidation of SO_3^{2-} by MnO_2 and is known to be stable.[33] In the present pH range of 3−4, $S_2O_6^{2-}$ should exist most probably in the monoprotonated form, $HS_2O_6^-$. Reaction 1 converts at least four protons into H_2O for one manganese ion. As can be seen in Figure 1, the OS region appears for $[Mn^{2+}]_0 > 4-5$ mM when $[H^+]_0 = 16.5$ mM is employed. Disappearance of OS for a lower value of $[Mn^{2+}]_0$ suggests that the manganese species is insufficient for consuming protons completely. This fact, together with the $[BrO_3^-]_0$ dependence and the results for MnO_4^- used in lieu of Mn^{2+} as discussed below, would suggest that reaction 1 is the relevant process for the negative-feedback scheme.

The proportionality of the low-pH period of oscillations to $1/[Mn^{2+}]_0$ can now be understood reasonably on the basis of reaction 1; namely, the rate of process 1 occurring in the low-pH region should be proportional to $[MnO(OH)^+]$, which, in turn, is proportional to $[Mn^{2+}]_0$ if reaction 2 proceeds quickly and stoichiometrically (see below for further discussions to support this view).

In Figure 3, the low-pH period increases with increasing $[BrO_3^-]_0$. Since the D channel reactions take place here, the rate should increase (and, thus, the period should decrease) with $[BrO_3^-]_0$. The most plausible explanation for this reverse dependence would be the competition between reaction 1 and reaction D. The fast drop of pH into the low-pH region is known to be the result of an autocatalytic increase of free protons due to the D channel. As long as the system stays in the low-pH region, process D continues to take place, consuming the externally supplied SO_3^{2-} and keeping the system acidic. On the other hand, process 1 is also taking place to reduce $[H^+]$ slowly until the system turns into the high-pH region. Both processes have HSO_3^- commonly as reactants. Therefore, if one increases $[BrO_3^-]_0$, more HSO_3^- is taken in the D channel reaction, which should decrease the rate of reaction 1, resulting in the elongation of the low-pH period.

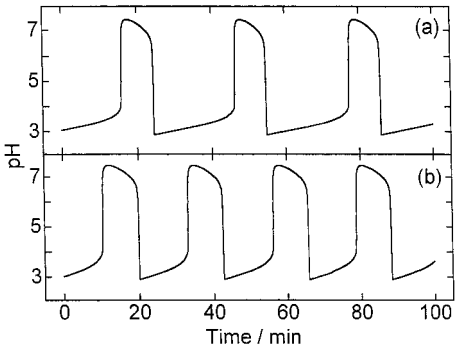

Figure 5. Measured pH oscillations in the $MnO_4^- - BrO_3^- - SO_3^{2-} - H^+$ system for the following $[MnO_4^-]_0$: (a) 1.5 and (b) 2.0 mM. The other parameters are fixed at $[H^+]_0 = 16.5$ mM, $[SO_3^{2-}]_0 = 118$ mM, $[BrO_3^-]_0 = 150$ mM, temperature = 45.0 °C, and the residence time = 7.02 min.

In the course of the experimental study, we have found large-amplitude oscillations in the system where Mn^{2+} is replaced by MnO_4^-, as shown in Figure 5. The system exhibits oscillations with relatively small $[MnO_4^-]_0$ compared with the case of Mn^{2+}. In addition, compared with Mn^{2+}, a more rapid decrease of the duration of the low-pH region and a slight increase of the high-pH region are observed for increasing $[MnO_4^-]_0$. The reaction mixture is colorless throughout the oscillations; the purple color characteristic of MnO_4^- disappears immediately at the tip of the inlet tube. Further increase of $[MnO_4^-]_0$ beyond 2.0 mM results in a bifurcation to the high-pH steady-state accompanied by a precipitation of MnO_2.

The rapid disappearance of MnO_4^- may be due to the reaction

$$2MnO_4^- + 6HSO_3^- + 7H^+ \rightarrow 2MnO(OH)^+ + 3HS_2O_6^- + 4H_2O \quad (3)$$

where $MnO(OH)^+$ undergoes further reaction (process 1). The overall reaction is obtained as (reaction 1) × 2 + (reaction 3):

$$2MnO_4^- + 10HSO_3^- + 11H^+ \rightarrow 2Mn^{2+} + 5HS_2O_6^- + 8H_2O \quad (4)$$

which may be compared with reaction 1. It is interesting to note that $^{21}/_2 = 10.5$ protons are consumed per one MnO_4^- in reaction 4, which may account for the experimental fact that ca. 1.5 mM of MnO_4^- is sufficient for oscillations to occur with $[H^+]_0 = 16.5$ mM. In contrast, reaction 1 in the Mn^{2+} system consumes four protons for one manganese as mentioned above. If the same stoichiometry is assumed to be applied to both cases, the minimum concentration of manganese required to induce oscillations in the Mn^{2+} system would be $1.5 \times {}^{10.5}/_4 \approx 4$ mM, which is close to the observed lower limit of $[Mn^{2+}]_0 \approx 4-5$ mM for oscillations to occur. Thus, the stoichiometry given in eqs 1 and 4 seems to account for the observation correctly.

We have performed a separate experiment to test the production of $MnO(OH)^+$ from Mn^{2+} given in reaction 2; in a

batch system, a mixture of 100 mM BrO_3^-, 10 mM H^+, and 1.0 mM Mn^{2+} remains unchanged for 50 min at room temperature. However, after 50 min, it turns yellow-brown with increasing rate and the reaction suddenly goes to completion in 5 min. This suggests that autocatalytic production of $MnO(OH)^+$ takes place as

$$MnO(OH)^+ + Mn^{2+} + H^+ \rightarrow 2Mn(OH)^{2+} \quad (5)$$

$$6Mn(OH)^{2+} + BrO_3^- + 3H_2O \rightarrow 6MnO(OH)^+ + Br^- + 6H^+ \quad (6)$$

where (reaction 5) × 3 + (reaction 6) gives reaction 2. Reaction 2 does not proceed if $[MnO(OH)^+] \approx 0$, while it proceeds autocatalytically once a trace of $MnO(OH)^+$ is produced. Presumably, in the low-pH region of OS in the Mn^{2+} system, $MnO(OH)^+$ is existent more or less and reaction 2 proceeds quickly throughout the low-pH period to keep $[MnO(OH)^+] \approx [Mn^{2+}]_0$.

The oscillatory waveforms for the Mn^{2+}-containing system (Figures 3 and 4) and for the MnO_4^--containing system (Figure 5) show a sharp decrease of pH leading to the low-pH region and a sharp increase of pH back to the high-pH region. The former is already clear, since it is known to be the result of autocatalytic production of H^+ due to the D channel reactions.[24] However, the latter has not been reported so far and requires some discussions. Although the sharp change is somewhat exaggerated in the logarithmic pH scale, the nonlinear character of the change is clear even in the $[H^+]$ scale (the change is $[H^+] = 0.13-0$ mM, compared with the high-pH-to-low-pH change of $[H^+] = 0-1.66$ mM). A possible mechanism responsible for this sharp change is the mode switching from the D channel into the S channel, where some extent of nonlinearity could be expected. However, if one compares the low-pH-to-high-pH transitions for the Mn^{2+} system and the MnO_4^- system, the pH turns more sharply for the former system at the end of the low-pH region. Although the reason for this difference is not clear at present, the nonlinearity brought about by the additional autocatalytic reaction (reaction 5) × 3 + (reaction 6) might be responsible for the sharper transition in the Mn^{2+} system, where externally supplied Mn^{2+}, as well as Mn^{2+} produced in reaction 1, is quickly converted to $MnO(OH)^+$ by the autocatalysis to keep $[MnO(OH)^+] \approx [Mn^{2+}]_0$. The apparent first-order rate constant (k') for H^+ consumption is kept constant to the very end of the low-pH region until the transition from the D channel to the S channel takes place. In contrast, Mn^{2+} is nonexistent initially in the MnO_4^- system. The rate of decrease of $[H^+]$ is determined predominantly by relatively slow production of $MnO(OH)^+$ from MnO_4^-, while, as the reaction proceeds, Mn^{2+} produced by reaction 1 is converted to $[MnO(OH)^+]$ autocatalytically to enhance the consumption of H^+ through step 1. Therefore, k' increases to the end of the low-pH stage. We are now trying to reproduce the processes by a computer simulation.

Conclusions

We observed large-amplitude regular pH oscillations in the $Mn^{2+}-BrO_3^--SO_3^{2-}-H^+$ system under flow conditions. Conditions for the stable pH oscillations were established on the control-parameter plane spanned by $[BrO_3^-]_0$ and $[Mn^{2+}]_0$, which exhibited a typical cross-shaped phase diagram. The autocatalytic production of H^+ is provided by the $BrO_3^--SO_3^{2-}-H^+$ subsystem, which is considered to be unaffected by the addition of Mn^{2+}. For the reaction mechanism responsible for the consumption of H^+, we proposed the reduction of $MnO(OH)^+$ by HSO_3^- to give $HS_2O_6^-$. The large-amplitude pH oscillations were also found for MnO_4^- used as a manganese source instead of Mn^{2+}. In this case, MnO_4^- is first reduced to $MnO(OH)^+$ and then undergoes the reaction with HSO_3^-. In both cases, the experimental conditions for the stable oscillations are consistent with the stoichiometry of the reduction of manganese species by HSO_3^-.

The oscillatory waveforms are distinct from any other pH oscillations reported so far in that the high-pH stage and the low-pH stage are well separated and that the transitions between them are extremely sharp in both directions. It has some resemblance to a pulse wave. Furthermore, durations of both high-pH and low-pH stages can easily be controlled over a wide range by choosing the input concentrations appropriately. In particular, the duration of the low-pH stage can be greatly lengthened. This has not been observed previously in other pH oscillators. The present pH oscillator systems are unique in that the bisulfite ion, HSO_3^-, plays a role as a key species to produce a nonlinearity *both* in the proton-producing and in the proton-consuming processes.

The discovery of manganese as a novel H^+-consuming species not only enriches the variety of the pH-oscillator family based on the $BrO_3^--SO_3^{2-}-H^+$ system but also provides the possibility of designing novel chaotic pH oscillators in combination with other H^+-consuming species. It would also be interesting to examine if the manganese catalyst is capable of consuming H^+ in other types of pH-clock reaction such as $IO_3^--SO_3^{2-}-H^+$ and $H_2O_2-SO_3^{2-}-H^+$. The use of manganese is advantageous over $Fe(CN)_6^{4-}$ or the granular marble used so far, since it is less harmful and easier to deal with. The present system would be suitable for a convenient visual demonstration if it is combined with appropriate pH indicators such as methyl orange or methyl red. Finally, we should emphasize good reproducibility and high controlability exhibited in the present system, which should provide a realistic basis for the possible application to bionics and biomedical engineering.[18−21]

Acknowledgment. N.O. thanks Professor Takeko Matsumura of Nara University of Education and Dr. Yoshihito Mori of Ochanomizu University for their continued encouragement.

References and Notes

(1) Orbán, M.; Epstein, I. R. *J. Am. Chem. Soc.* **1985**, *107*, 2302.
(2) Rábai, G.; Orbán, M.; Epstein, I. R. *Acc. Chem. Res.* **1990**, *23*, 258.
(3) Luo, Y.; Epstein, I. R. *J. Am. Chem. Soc.* **1991**, *113*, 1518.
(4) Lee, K. J.; McCormick, W. D.; Quyang, Q.; Swinney, H. L. *Science* **1993**, *261*, 192.
(5) Lee, K. J.; McCormick, W. D.; Pearson, J. E.; Swinney, H. L. *Nature* **1994**, *369*, 215.
(6) Keresztessy, A.; Nagy, I. P.; Bazsa, G.; Pojman, J. A. *J. Phys. Chem.* **1995**, *99*, 5379.
(7) Nagy, I. P.; Keresztessy, A.; Pojman, J. A. *J. Phys. Chem.* **1995**, *99*, 5385.
(8) Rábai, G.; Kustin, K.; Epstein, I. R. *J. Am. Chem. Soc.* **1989**, *111*, 8271.
(9) Mori, Y.; Hanazaki, I. *J. Phys. Chem.* **1992**, *96*, 9083.
(10) Mori, Y.; Hanazaki, I. *J. Phys. Chem.* **1993**, *97*, 7375.
(11) Vanag, V. K.; Mori, Y.; Hanazaki, I. *J. Phys. Chem.* **1994**, *98*, 8392.
(12) Kaminaga, A.; Rábai, G.; Mori, Y.; Hanazaki, I. *J. Phys. Chem.* **1996**, *100*, 9389.
(13) Kaminaga, A.; Rábai, G.; Hanazaki, I. *Chem. Phys. Lett.* **1998**, *284*, 109.
(14) Rábai, G.; Kaminaga, A.; Hanazaki, I. *J. Chem. Soc., Chem. Commun.* **1996**, 2181.
(15) Rábai, G.; Hanazaki, I. *J. Phys. Chem.* **1996**, *100*, 15454.
(16) Rábai, G. *J. Phys. Chem. A* **1997**, *101*, 7085.
(17) Rábai, G.; Hanazaki, I. *J. Am. Chem.* Soc. **1997**, *119*, 1458.

(18) Giannos, S. A.; Dinh, S. M.; Berner, B. *Macromol. Rapid Commun*. **1995**, *16*, 527.
(19) Giannos, S. A.; Dinh, S. M.; Berner, B. *J. Pharm. Sci.* **1995**, *84*, 539.
(20) Siegel, R. A.; Zou, X.; Baker, J. P. *Proc. Int. Symp. Controlled Release Bioactive Mater*. **1996**, *23*, 115.
(21) Yoshida, R.; Ichijo, H.; Hakuta, T.; Yamaguchi, T. *Macromol. Rapid Commun*. **1995**, *16*, 305.
(22) Edblom, E. C.; Luo, Y.; Orbán, M.; Kustin, K.; Epstein, I. R. *J. Phys. Chem.* **1989**, *93*, 2722.
(23) Rábai, G.; Kaminaga, A.; Hanazaki, I. *J. Phys. Chem*. **1996**, *100*, 16441.
(24) Hanazaki, I.; Rábai, G. *J. Chem. Phys.* **1996**, *105*, 9912.
(25) Williamson, F. S.; King, E. L. *J. Am. Chem. Soc*. **1957**, *79*, 5397.
(26) Szirovicza, L.; Boga, E. *Int. J. Chem. Kinet*. **1998**, *30*, 869.
(27) Rábai, G.; Hanazaki, I. *J. Phys. Chem.* **1996**, *100*, 10615.
(28) Okazaki, N.; Hanazaki, I. *J. Chem. Phys*. **1998**, *109*, 637.
(29) De Kepper, P.; Epstein, I. R.; Kustin, K. *J. Am. Chem. Soc*. **1981**, *103*, 6121.
(30) De Kepper, P.; Boissonade, J. In *Oscillations and Traveling Waves in Chemical Systems*; Field, R. J., Burger, M., Eds.; Wiley-Interscience: New York, 1985; p 223.
(31) Edblom, E. C.; Orbán, M.; Epstein, I. R. *J. Am. Chem. Soc.* **1986**, *108*, 2826.
(32) Orbán, M.; Lengyel, I.; Epstein, I. R. *J. Am. Chem. Soc.* **1991**, *113*, 1978.
(33) Cotton, F. A.; Wilkinson, G. In *Advanced Inorganic Chemistry*, 5th ed.; Wiley-Interscience: New York, 1988; p 523.